ISSN 1070-4272, Russian Journal of Applied Chemistry, 2017, Vol. 90, No. 4, pp. 613−624. © Pleiades Publishing, Ltd., 2017.

VARIOUS TECHNOLOGICAL PROCESSES

Electropolymerization, Characterization and Corrosion Protection Evolution of Poly(4-aminomethyl-5-hydroxymethyl-2-methylpyridine-3-ol) on Steel and Copper[1]

O. A. Abdullatef*

Faculty of Pharmacy & Drug Manufacturing, Pharos University, Alexandria, Egypt
**e-mail: ossama.abdullatef@pua.edu.eg*

Received April 9, 2017

Abstract—The electrochemical synthesis of poly(4-aminomethyl-5-hydroxymethyl-2-methyl pyridine-3-ol) on steel and copper electrodes was achieved in both sulfuric acid and oxalic acid by cyclic voltammetry technique. Characterization of the polymer films were achieved by Fourier transforms infrared spectroscopy technique (FTIR) and scanning electron microscope (SEM). Corrosion performance of coatings was investigated in 0.1 M H_2SO_4 by potentiodynamic polarization and electrochemical impedance (EIS) spectroscopy techniques.

DOI: 10.1134/S1070427217040188

INTRODUCTION

Since the revolutionary discovery, up to date, conducting polymers have received significant attention of researchers from both science and engineering communities. Its importance comes from their extraordinary electric and electronic applications [1–8]. Conducting polymers find many applications in industry, in corrosion protection, sensors, energy storage devices, electronic instruments [9–13]. General speaking, they are synthesized by either chemical or electrochemical oxidative polymerization [14, 15]. Conducting polymers which are synthesized chemically are important when we need a large amount of polymer. However, electrochemical polymerization takes first priority when the polymer film properties are important. In this type of polymerization the polymer is deposited on the metal surface. By adjusting the electrochemical polymerization process, the polymer film thickness and conductivity can be controlled [16]. Among the numerous known conducting polymers, polyaniline (PANI) was extensively studied due to its unique properties, such as electrical and optical activity and stability [17–22]**.** Conducting polymers other than polyaniline are also studied and find many applications in industry. Polypyrrole [23], poly(*N*-ethylaniline) [24], poly-*O*-phenylene diamine [25], polythiophene and its bilayer of PANI and PPy [26, 27] were intensively studied with respect to their electrochemical synthesis, characterization and corrosion performance. The corrosion performance studies regarding conducting polymers are based on decreasing the electrodissolution of metal at the very beginning of electropolymerization process [28] and formation of protective film on it. The aim of this study is electrochemical polymerization, characterization and corrosion protection evaluation of poly (4-aminomethyl-5-hydroxymethyl-2-methylpyridine-3-ol) which is commonly named as pyridoxamine hydrochloride on steel and copper metals. The anti-corrosion performance of these conducting polymers is investigated by potentiodynamic polarization and electrochemical impedance spectroscopy (EIS).

EXPERIMENTAL

Chemicals and apparatus. Pyridoxamine hydrochloride which is the common name of 4-aminomethyl-5- hydroxymethyl-2-methylpyridine-3-ol, oxalic acid and sulfuric acid used in this study were all purchased from Sigma Chemical Company. The pyridoxamine hydrochloride was used without any further purifica-

[1] The text was submitted by the author in English.

tion. All electrochemical polymerization experiments were performed in aqueous solution of 1×10^{-4} M pyridoxamine hydrochloride, abbreviated as POX, in either 0.1 M H_2SO_4 or 0.1 M oxalic acid using double distilled water. All experiments were performed at 30°C. Electro synthesis and electrochemical studies were carried out in a three electrode system with copper or steel as working electrodes, platinum sheet was used as counter electrode, and calomel electrode (SCE) was used as the reference electrode. The working electrode was constructed from a copper or steel rod of 0.6 mm diameter embedded in Teflon holder. The chemical composition of the copper electrode (wt %) is Cu^{+2} 99.5; Ca 0.5; and the steel electrode C 0.21; S 0.04; Mn 2.5; P 0.04; Si 0.35; balance Fe. Prior to each experiment the working electrodes were polished using a series of emery papers (300, 800, and 1000 grades) and cleaned with distilled water and ethanol and then dried in air. ACM 604 Potentiostate instrument was used for electrochemical synthesis and corrosion performance studies. The analysis of the impedance spectra were performed by Zisimpwin 3.2 program by fitting the experimental data to the appropriate equivalent circuit.

Preparation of polypyridoxamine hydrochloride (PPOX) coat on Cu and Fe electrodes. The PPOX coatings were synthesized by electrochemical polymerization of pyridoxamine hydrochloride (POX) on Cu and Fe substrates from aqueous solutions containing either 0.1 M oxalic acid or 0.1 M sulfuric acid using cyclic voltammetry in two different potential ranges (–0.8 V to 1.4 V in case of oxalic acid, and –0.4 V to 1.4 V in case of sulfuric acid) vs. SCE at scan rate of 1800 mV min^{-1} for Fe and 600 mV min^{-1} for Cu over 10 cycles for Cu and 20 cycles for Fe. After electrodeposition of PPOX coats, the polymer coated electrodes were removed from the electropolymerization medium and rinsed with double distilled water to remove monomer molecules and being dried in air.

Charaterization of PPOX coats. The structures of both monomer and PPOX polymers were analyzed by FTIR spectrophotometry using TENSOR 37 Bruker model infrared spectrophotometer. The morphologies of the PPOX polymers were investigated by scanning electron microscope (SEM) using JOEL instrument.

Corrosion performance measurements. Corrosion performance of coated and uncoated copper and steel electrodes was carried out in aqueous solution of 0.1 M H_2SO_4 by potentiodynamic polarization and electrochemical impedance spectroscopy (EIS) measurements. The polarization curves were recorded by charging the electrode potential between –250 mV and +500 mV with constant sweep rate 1200 mV min^{-1}. The frequency range of impedance spectra is 30 kHz to 10 mHz using AC amplitude of 10 mV.

RESULTS AND DISCUSSION

It is well known that electrochemical polymerization process is mainly consist of three steps, first of all, oxidation of the monomer at the anode leading to the formation of soluble oligomers in the diffusion layer, in the second step, deposition of oligomers on substrate through nucleation and growth formation and finally in the third step chain propagation by solid state polymerization [14].

Electropolymerization of POX Coat on Copper Electrode

Electropolymerization of POX monomer on Cu electrode from aqueous solution containing either 0.1 M H_2SO_4 or 0.1 M oxalic acid was done by cyclic voltammetry. Figure 1 shows the cyclic voltammograms during electropolymerization of POX on Cu electrode in 0.1 M H_2SO_4 solution by sweeping the potential in the region between –400 to +1400 mV at a scan rate of 600 mV min^{-1}. As can be seen from the first scan, an oxidation wave starts at about 200 mV which can be attributed to the oxidation of monomer. The intensity of this oxidation wave gradually decreases during the following scans and the oxidation potential shifts to higher potentials which indicates the electropolymerization of POX. This behavior confirmed the facts that have been mentioned before [14] which is deposition of oligomers on substrate through nucleation and growth formation and finally in the third step chain propagation by solid state polymerization. Starting with the second scan a reduction peak appears at –50 mV which can be attributed to the reduction of PPOX. This peak decreases in intensity as the PPOX coat grows with successive scans indicating that the polymer is well grown at this stage. At the end of the 10th cycle a brown PPOX coat becomes visible.

Figure 2 shows the cyclic voltammograms during electropolymerization of POX on Cu electrode in the presence of 0.1 M oxalic acid solution by sweeping the potential in the region between –800 mV to +1400 mV

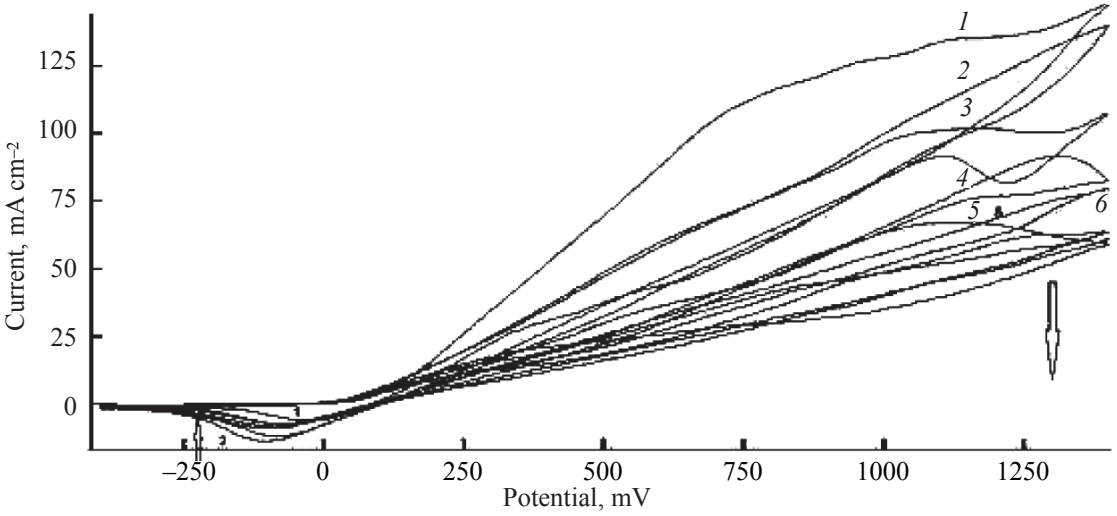

Fig. 1. The cyclic voltammograms recorded for Cu electrode in 0.1 M H_2SO_4 and 1×10^{-4} M POX.

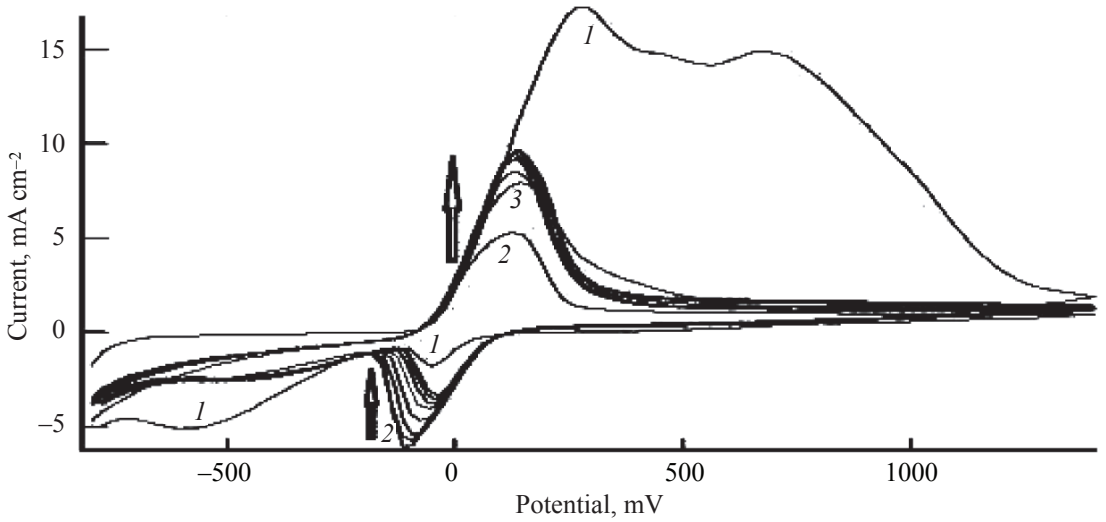

Fig. 2. The cyclic voltammograms recorded for Cu electrode in 0.1 M oxalic acid and 1×10^{-4} M POX.

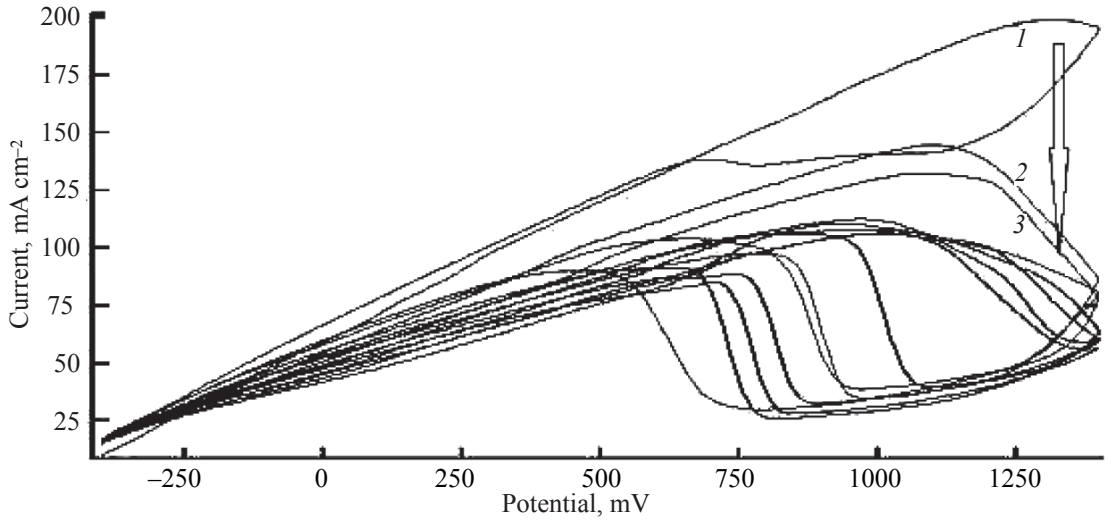

Fig. 3. The cyclic voltammograms recorded for Fe electrode in 0.1 M H_2SO_4 and 1×10^{-4} M POX.

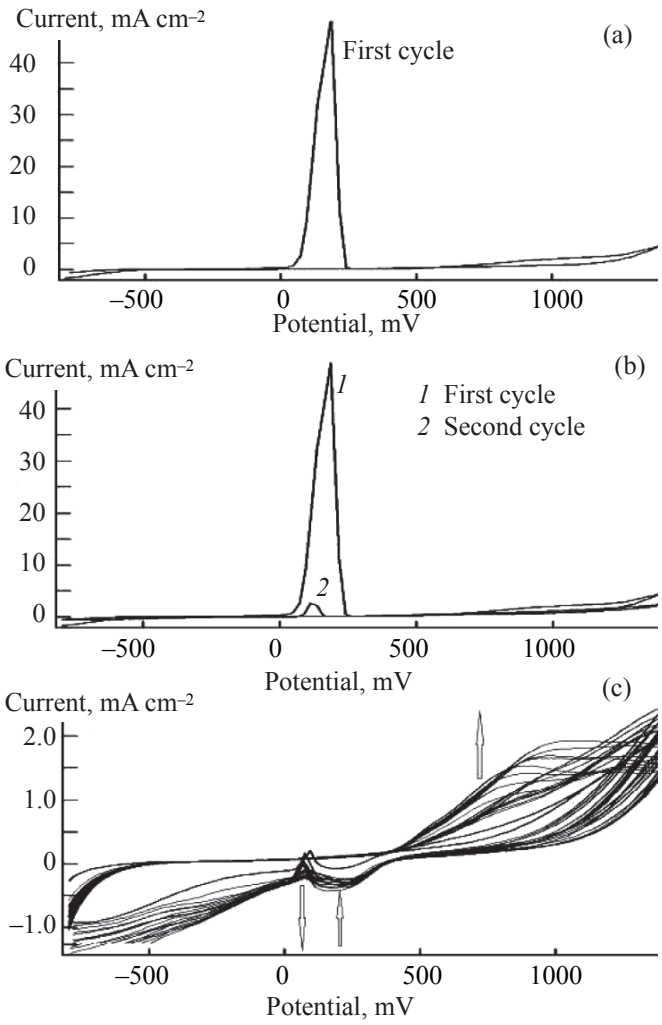

Fig. 4. The cyclic voltammograms recorded for Fe electrode in 0.1 M oxalic acid and 1 × 10–4 M POX (a) first cycle; (b) first and second cycles; (c) third to twentieth cycles.

at a scan rate 1800 mV min–1. The formation and growth of the polymer on Cu electrode can easily be followed by noticing the subsequent scans. The forward first scan showed two broad oxidation peaks at 300 and 700 mV which can be attributed to the oxidation of monomer POX, the first peak can be explained on the basis of the formation of monomer cation radical and the second peak suggests the formation of oligomers on the Cu electrode. During the subsequent scans, only one oxidation peak appears at 150 mV which increases in intensity with increasing the number of scans. On the other hand, the reduction peak at –50 mV shifted to more negative potential in the second reverse scan and the intensity decreases by increasing the number of scans which means that the rate of reduction of polymer decreases with the number of scans. The increasing intensity of the oxidation peak with subsequent scans while decreasing the reduction peak, which is opposite to what was expected, indicates the oxidation of the polymer after formation which may result in deterioration of the polymer film after growth. This can be an indication of the weak adherence of the PPOX which is formed in the presence of oxalic acid.

Electropolymerization of POX Coat on Steel Electrode

Figure 3 shows the cyclic voltammograms during electropolymerization of POX on Fe electrode in the presence of 0.1 M H_2SO_4 acid solution by sweeping the potential in the range between –400 mV to +1400 mV at a scan rate 600 mV min–1. Inspection of the cyclic voltammograms show that an oxidation broad band starts at about 650 mV indicating oxidative polymerization of the POX on the steel substrate. The same behavior was observed for all the subsequent scans in which the current density decreases gradually with the subsequent scans indicating the insulating effect of the deposited polymer on the steel substrate. In the meantime, there is no reduction peaks observed during the reverse scans indicating that the polymer formed is inert and cannot undergo reduction simultaneously with the oxidation process. This idea is confirmed by the corrosion measurements which will be explained later. Figure 4 shows the cyclic voltammograms during electropolymerization of POX on Fe electrode in the presence of 0.1 M oxalic acid solution by sweeping the potential between –800 mV to 1400 mV at a scan rate 1800 mV min–1. Figure 4a shows the first scan only, 4b shows the first and second scans and 4c from the 3rd to the 20th cycles. A large peak is observed at 186.2 mV during the forward scan of the first cycle which can be explained by assuming the dissolution of carbon steel in oxalic acid. The intensity of this peak decreases in the second cycle and nearly disappeared in the third cycle indicating that the dissolution of iron in oxalic acid decreased and nearly stopped at the third scan. Starting from the 10th cycle a broad oxidation peak appears at 790 mV which can be attributed to the oxidation of monomer on steel surface forming PPOX. In the meantime, a reduction peak appears at 203.3 mV which can be attributed to the reduction of polymer, this peak decreases in intensity with increasing the number of cycles indicating no more reduction of polymer. The increase in oxidation peak intensity in the meantime of decreasing the intensity of the reduction peak can be explained similar to that previously said during the discussion of the polymerization of POX on Cu metal

Table 1. Potentidynamic Polarization parameters of uncoated and coated Fe electrode in 0.1 M H_2SO_4

	$-E_{corr}$, mV	β_a, mV dec^{-1}	β_c, mV dec^{-1}	i_{corr}, mA cm^{-2}	P, %
Uncoated steel	507	117.7	100.2	0.9837	–
Coated steel in the presence of H_2SO_4	95.5	113.6	167.7	0.0087	99.1
Coated steel in the presence of oxalic acid	545	89.3	107.2	0.4127	58.0

in the presence of oxalic acid. The above mentioned discussion directed to the conclusion that the PPOX film is well formed and well adhered if it is synthesized in the presence of sulfuric acid. On the other hand, a weak film which is weakly adhered to the surface will be formed if it is synthesized in the presence of oxalic acid. These facts will be confirmed by the corrosion performance evaluation of the PPOX on Cu and Fe which will be discussed later.

Corrosion Protection Performance of PPOX Coatings

The corrosion protection efficiencies of PPOX coatings electropolymerized on Cu and Fe were tested in 0.1 M H_2SO_4 solution by using potentiodynamic polarization and electrochemical impedance spectroscopy (EIS) techniques.

Potentiodynamic polarization measurements. The polarization curves recorded in 0.1 M H_2SO_4 for uncoated and coated Cu by PPOX which is synthesized in the presence of either 0.1 M H_2SO_4 or 0.1 M oxalic acid are given in Fig. 5. Inspection of the polarization curves showed that the PPOX coat shifts the corrosion potential to more positive potential compared to bare metal. In the same time, it has predominate effect on the cathodic reaction and a little effect on the anodic part.

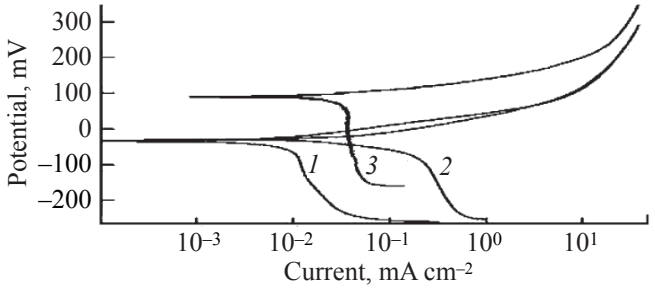

Fig. 5. Tafel curves recorded in 0.1 M H_2SO_4 for uncoated and coated Cu electrodes by PPOX synthesized in the presence of oxalic acid and sulfuric acid.

The cathodic parts of the polarization curves show limiting current corresponds to the oxygen reduction reaction that is slightly affected by the coat which cannot be analyzed using Tafel extrapolation. This indicates that the cathodic process is controlled by diffusion of oxygen gas from the bulk solution to the metal surface. This behavior is well known since copper can hardly be corroded in the deoxygenated dilute sulfuric acid [29], as copper cannot displace hydrogen from acid solutions according to the theories of chemical thermodynamics. However, in aerated sulfuric acid, dissolved oxygen is reduced on copper surface and this will enable some corrosion to take place [30]. Cathodic reduction of oxygen can be expressed either by two consecutive 2*e*-steps involving a reduction to hydrogen peroxide first followed

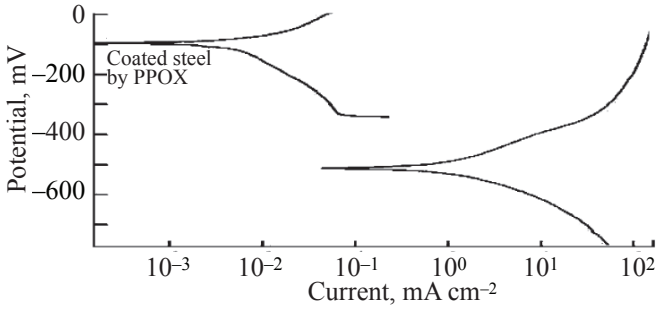

Fig. 6. Tafel curves recorded in 0.1 M H_2SO_4 for uncoated and coated Fe electrodes by PPOX synthesized in sulfuric acid.

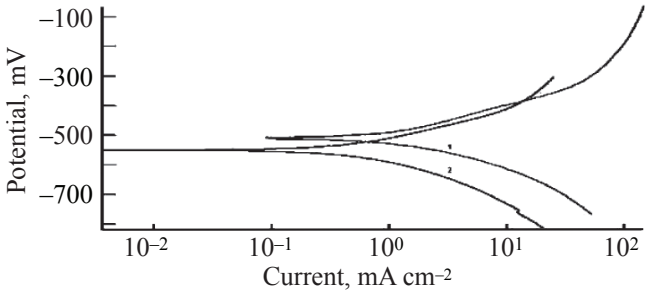

Fig. 7. Tafel curves recorded in 0.1 M H_2SO_4 for uncoated and coated Fe electrodes by PPOX synthesized in oxalic acid. (*1*) Uncoated steel, (*2*) coated steel in the presence of oxalic acid.

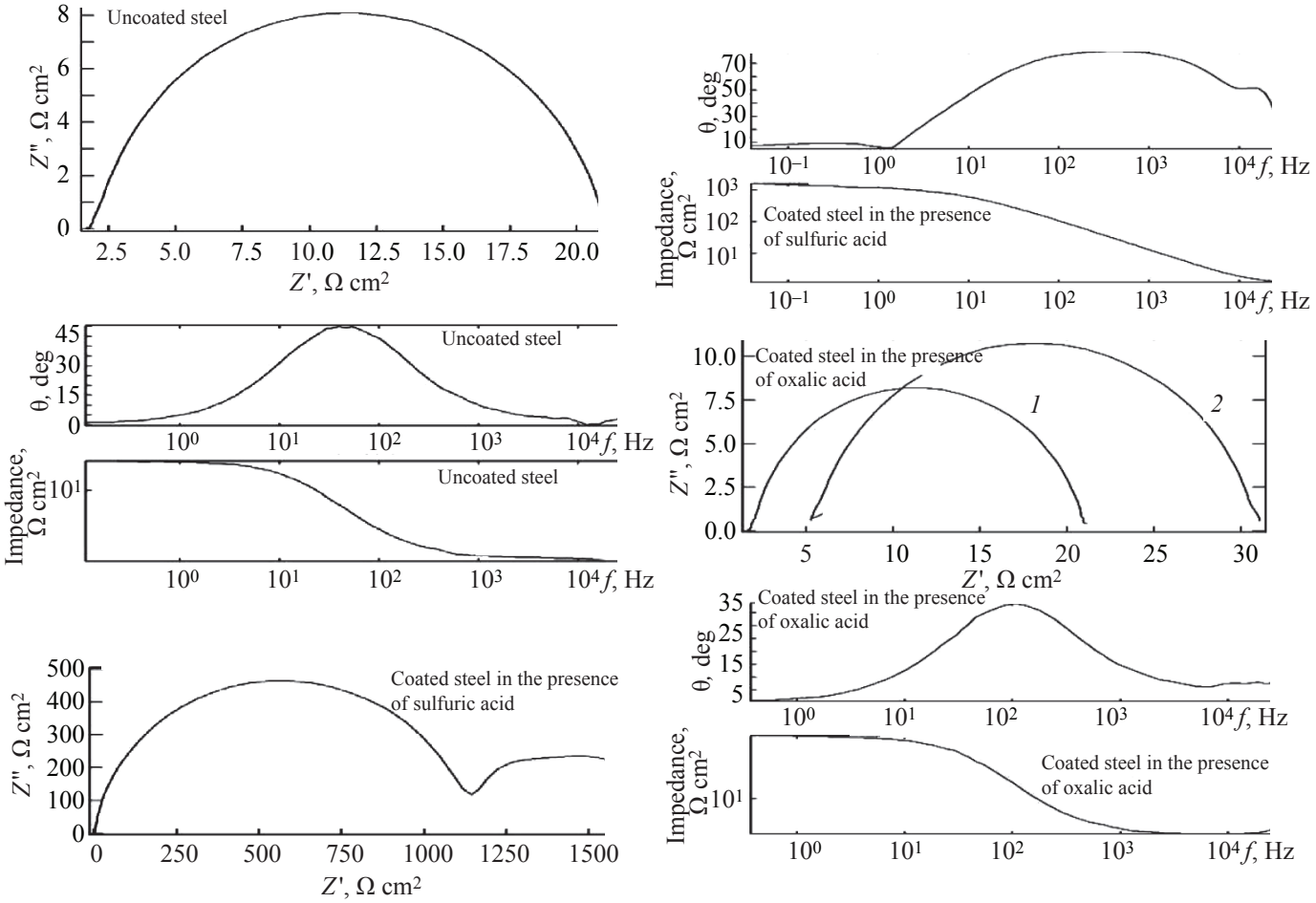

Fig. 8. (a) Nyquist plots for uncoated steel recorded in 0.1 M H_2SO_4; (b) Bode and Theta plots for uncoated steel recorded in 0.1 M H_2SO_4; (c) Nyquist plots for coated steel in the presence of sulfuric acid; (d) Bode and Theta plots for coated steel in the presence of sulfuric acid; (e) Nyquist plots for coated steel in the presence of oxalic acid; (f) Bode and Theta plots for coated steel in the presence of oxalic acid. (*1*) Uncoated steel, (*2*) coated steel in the presence of oxalic acid. (*f*) Frequency.

by a further reduction to water or by a direct 4*e*-transfer step [31] as shown by the equation:

$$O_2 + 4H^+ + 4e^- \leftrightarrows 2H_2O$$

The coated copper in the presence of H_2SO_4 affects the values of corrosion potential and shifts it to more positive values indicating that this type of coat inhibit the corrosion of copper. The anodic part of the polarization curves for coated copper shows Tafel behavior indicating that the oxidation process is mainly controlled by charge transfer. It was reported before that the anodic dissolution of copper in acidic solutions can be illustrated by the following two consecutive steps [32]:

$$Cu \leftrightarrows Cu^+_{ads} + e^-, \text{ (fast)}$$

$$Cu^+_{ads} \leftrightarrows Cu^{2+}_{sol} + e^-, \text{ (slow)}$$

Regarding the cathodic reaction in the presence of coated copper; the surface includes an easily reducible polymer. So, an additional cathodic reaction involves the reduction of the PPOX polymer. This reaction must predominate the oxygen or water reduction at cathodic areas. The polarization curves recorded in 0.1 M H_2SO_4 for uncoated and coated steel by PPOX polymerized an acid are given in Figs. 6 and 7, respectively. The figures show that the coat affected both the cathodic and anodic Tafel lines indicating that the PPOX coat decreases the rate of both the cathodic and anodic reactions. The values of E_{corr}, i_{corr}, β_a, and β_c (Tafel constants), and the protection efficiency are given in Table 1. The protection efficiency was calculated using the following relation:

$$P, \% = [(i_{a0} - i_a)/i_{a0}] \times 100,$$

where; i_{a0} and i_a are the anodic currents in the presence of uncoated and coated steel, respectively. As can be seen, a decrease in i_{corr} in case of coated Fe than in case of uncoated Fe indicates that the coat decreases the rate of corrosion reaction. The fact that i_{corr} is less in case of coated steel in the presence of sulfuric acid than in the presence of oxalic acid indicating that the PPOX coat is more protective if it is polymerized in the presence of H_2SO_4 and has the potential to decrease the corrosion rate of steel in 0.1 M H_2SO_4. The clear observation of changed values of Tafel constants β_a and β_c indicates that the polymer film acts as a barrier for both cathodic and anodic reactions by decreasing the surface area available for both reactions.

Electrochemical impedance measurements. The electrochemical impedance spectroscopy (EIS) recorded in 0.1 M H_2SO_4 solution was used to analyze the (Electrode/PPOX/Electrolyte) system of both steel and copper coated by PPOX polymer synthesized in the presence of either oxalic acid or sulfuric acid solution. The electrochemical parameters of the coated electrode/electrolyte systems were evaluated by employing the ZSimpWin software. Good agreement between the experimental results and the parameters obtained from the $R(Q(R(Q(RW))))$ equivalent circuit model for coated copper (in sulfuric acid)/electrolyte system represented in Fig. 10c, $R(Q(R(Q(RW))))$ and for coated steel (in the presence of sulfuric acid)/electrolyte system represented in Fig. 10b and $R(CR)$ equivalent circuit model for uncoated electrode/electrolyte and coated steel in the presence of oxalic acid represented in Fig. 10a, where the chi-square (χ^2), which represent the discrepancy between the experimental results and the fitting results, is minimized from 0.00217 to 0.001265 value. The uncoated equivalent circuit model which is represented in Fig. 10a was built using series components; the first is the bulk solution resistance of the electrolyte R_s; the second is the parallel combination of the capacitance of double layer C_{dl} and the charge transfer resistance R_{ct}. The coated equivalent circuit model which is represented in Fig. 10b was built using series components; the first is the bulk solution resistance of the electrolyte R_s; the second is the parallel combination of the capacitance of the polymer coating C_p and the coating resistance R_p. Another parallel combination, built in series to R_p, which is the capacitance of the double layer C_{dl} and R_{ct} which is the charge transfer resistance. The equivalent circuit model which is represented in Fig. 10c is similar to that in 10b except the Warburg constant which is added in series to the charge transfer resistance. The constant phase element (CPE) is introduced in the equivalent circuit instead of the pure capacitor of the double layer C_{dl} in the fitting procedure to obtain good agreement between

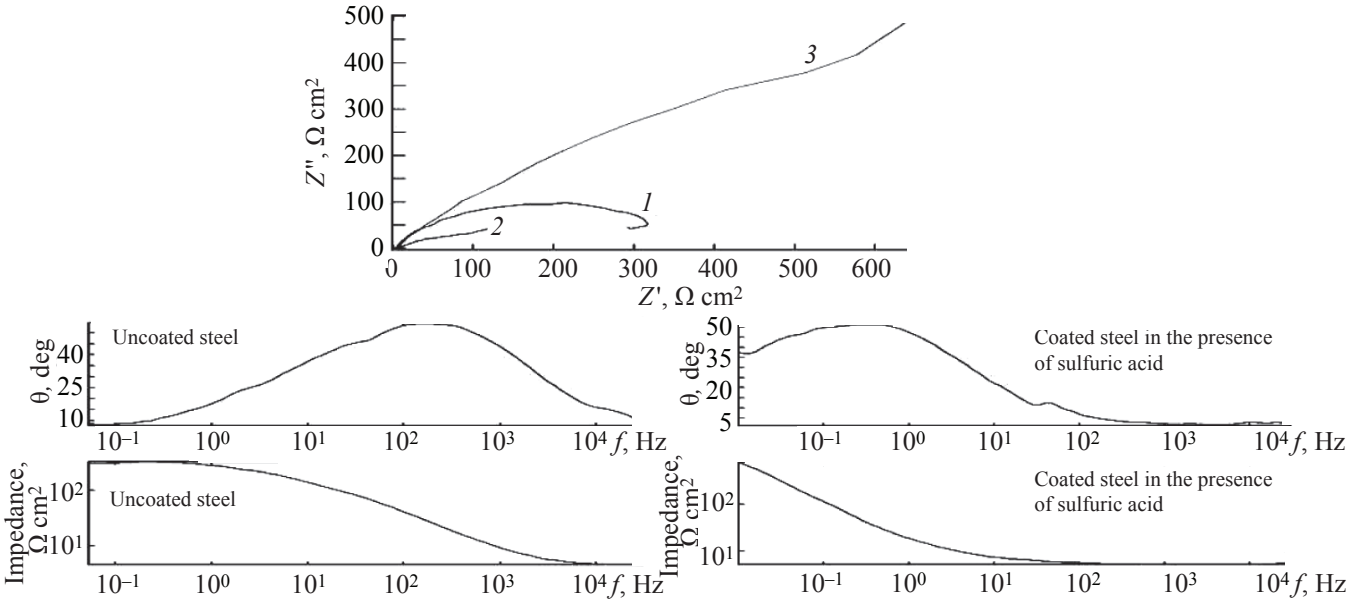

Fig. 9. (a) Nyquist plots for uncoated and coated copper by PPOX recorded in 0.1 M H_2SO_4; (b) Bode and Theta plots for uncoated copper recorded in 0.1 M H_2SO_4; (c) Bode and Theta plots for coated copper synthesized in sulfuric acid solution, recorded in 0.1 M H_2SO_4. (*1*) Uncoated steel, (*2*) coated steel in the presence of sulfuric acid, (*3*) coated steel in the presence of oxalic acid. (*f*) Frequency.

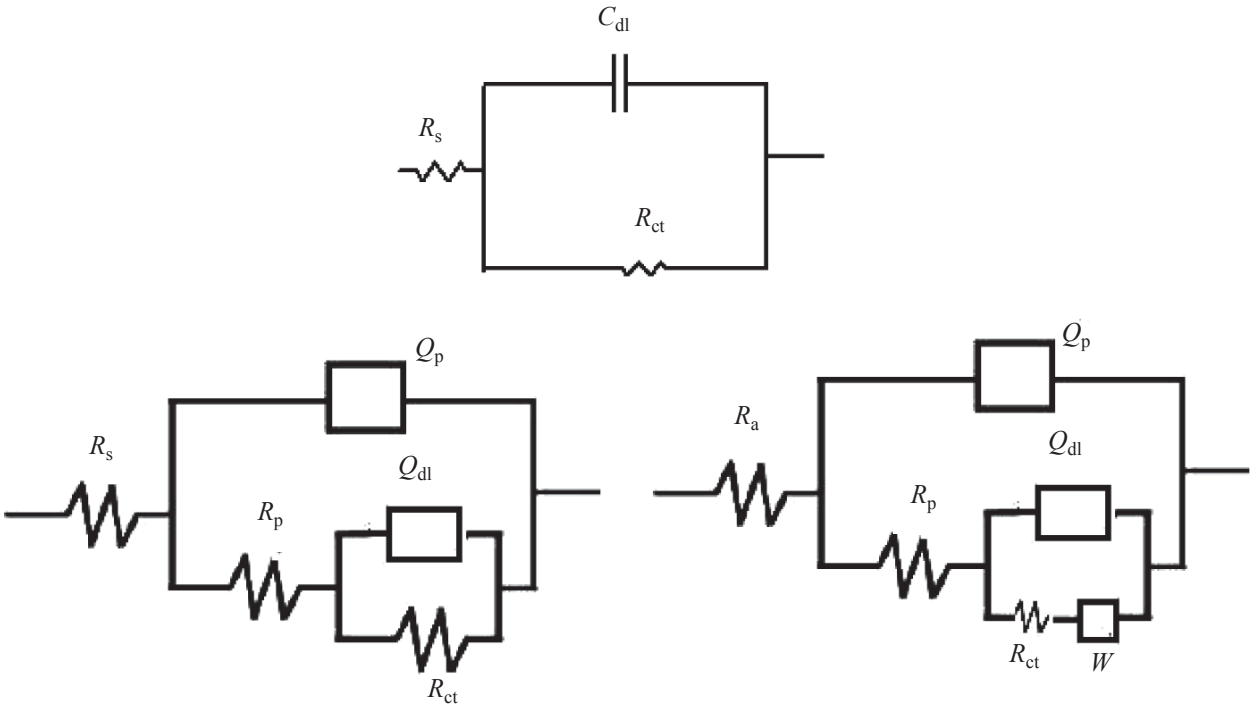

Fig. 10. Equivalent circuits used to fit the experimental results.

the simulated and experimental results. Figures 8 and 9 show the Nyquist plots of the uncoated and coated steel and copper. It can be seen that the Nyquist plots for the uncoated steel and copper (Figs. 8a and 9a) consist of only one depressed semicircle while the Nyquist plots for the coated steel and copper (Figs. 8c, 8e, and 9a) consist of two semicircles; the first one at high frequencies represent the coating resistance and the second one at low frequencies represent the charge transfer resistance. The CPE in case of coated steel and copper can be presented by the parameter Q and the exponent n. Q is used to compensate for non-homogeneity in the system and is defined by two values, C and n where; $0 \le n \le 1$. Note that for a value of $n = 1$, the Q value corresponds to the capacitance, for $n = 0$, a resistance and for $n = 0.5$ a Warburg element. Simulation results for uncoated and coated steel and copper electrolyte system are given in Table 2. Inspection of the Nyquist plots indicates that PPOX coatings have considerable protective behavior if the POX is polymerized in the presence of H_2SO_4 while in the presence of oxalic acid it has acceleration behavior. The electrochemical impedance parameters and the protection efficiency are given in Table 2. The protection efficiency is calculated from the following equation:

$$P, \% = [(R_{CT} - R_{CT0})/R_{CT}] \times 100,$$

where R_{CT0} and R_{CT} are the charge transfer resistances in the coated and uncoated Fe and Cu. The results showed that R_{CT} values for coated steel and copper are higher than that for uncoated steel and copper suggests the formation of a protective layer of the PPOX coat. The protective film act as a barrier for mass and charge transfer. The low values of R_{CT} in case of PPOX coats that was synthesized in the presence of oxalic acid indicated that the polymer is not protective if it is synthesized in the presence of oxalic acid. The fact that the PPOX coat polymerized in the the presence of H_2SO_4 acts as protective layer is confirmed by the high values of the protection efficiency obtained.

Characterization of the PPOX Coats

IR. In order to elucidate the structure of the PPOX coat FT-IR spectra was recorded in the range 675–4000 cm^{-1}. For comparison, the spectrum of the monomer was also included in the figure. It is previously reported that polymerization is confirmed by modifications appeared in the polymerization. Thus, some characteristic bands from the monomer are maintained, while shifting of some peaks in their intensity and width take place and some new peaks appeared. Figure 11 represents the FTIR spectrum for POX, PPOX coated in the presence of sulfuric acid formed on Cu and Fe electrodes respectively. It is clear

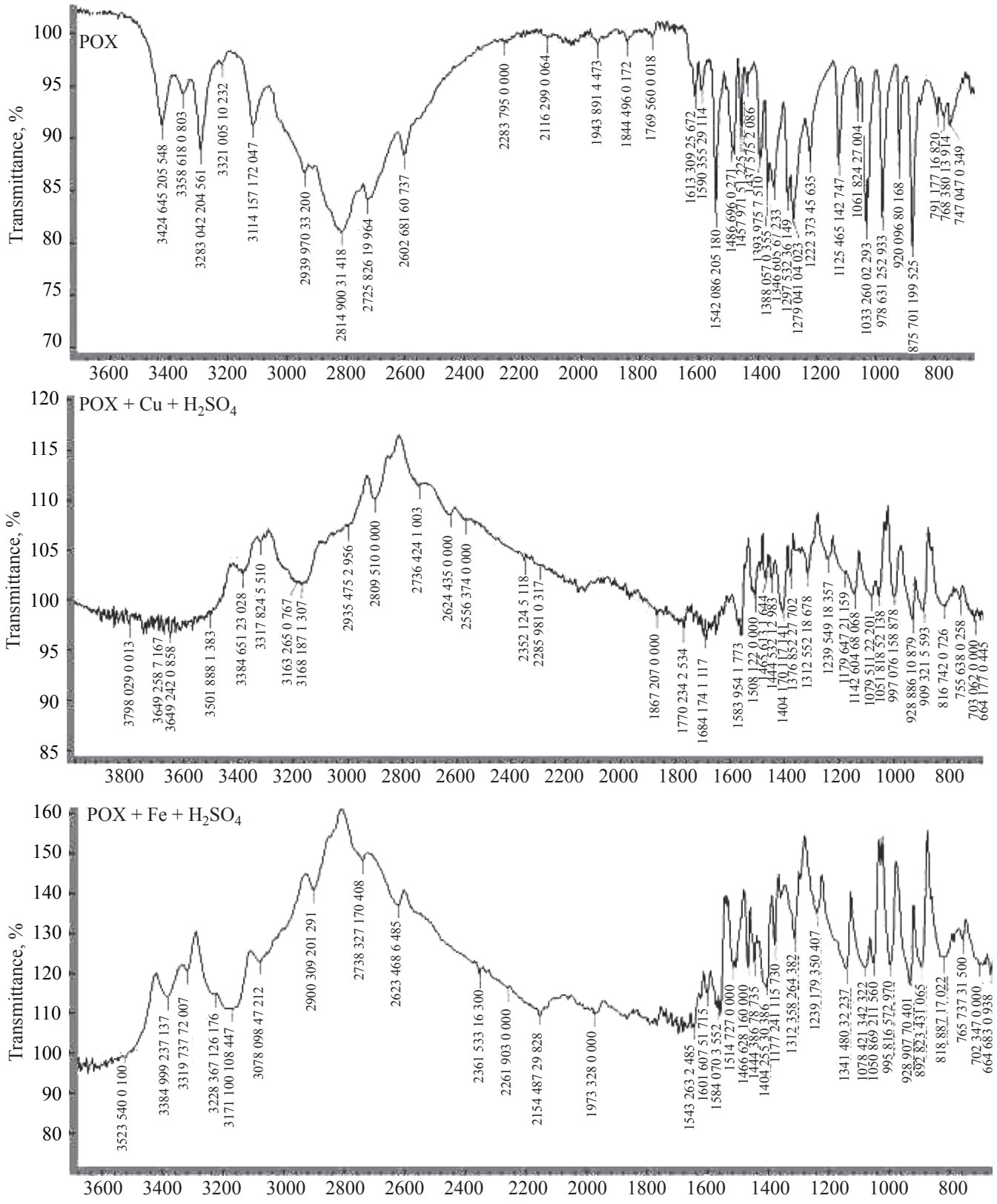

Fig. 11. Infrared spectra of polymer films formed at Cu and Fe electrodes by PPOX, (a) POX monomer; (b) POX on Cu; (c) POX on Fe.

Table 2. Impedance parameters of uncoated and coated Fe and Cu electrodes in 0.1 M H_2SO_4

Sample	R_s, Ω cm^2				C_{dl}, F		R_{CT}, Ω cm^2	P, %	W
Uncoated steel	1.5				9.5×10^{-3}		19.5	–	
Sample	R_s, Ω cm^2	Q_p, F	n	R_p	Q_{dl}, F	n	R_{CT}, Ω cm^2	P, %	W
Coated steel in the presence of H_2SO_4	0.88	2.998×10^{-5}	0.47	1131	1.229×10^{-3}	0.43	814.9	97.6	
Coated steel in the presence of oxalic acid	5.1				3.110×10^{-3}		26	33.3	
Uncoated copper	3.8				3.7×10^{-3}		308	–	
Coated copper in the presence of H_2SO_4	4.4	2.038×10^{-4}	0.82	4.8	1.793×10^{-2}	0.36	2131	85.6	1.53×10^7
Coated copper in the presence of oxalic acid	5.3	5.102×10^{-3}	0.86	8.4	6.123×10^{-3}	0.87	81.3	–	3.50×10^6

from Fig. 11, that some modifications appear in the polymerization process. Inspection of the IR spectra showed that, a peak at 3424 cm^{-1} seen in the monomer spectra and not found in the polymer spectra corresponds to the N–H stretching vibration. The peak at 3353 cm^{-1} in the monomer spectra shifted to 3384 cm^{-1} in the polymer spectra corresponds to the hydrogen bonded O–H. The peak at 3293 cm^{-1} seen in the monomer spectra and not found in the polymer spectra corresponds to the non-hydrogen bonded O–H. The disappearance of the N–H peak at 3424 cm^{-1} and O–H peak at 3293 cm^{-1} indicates that both N–H and O–H function groups participate in the polymerization**.** The peak at 3114 cm^{-1} in the monomer spectra shifted to 3183–3171 cm^{-1} in the polymer spectra corresponds to the C–H aromatic bond. The peak at 2939 cm^{-1} in the monomer spectra shifted to 2900 cm^{-1} in the polymer spectra corresponds to the C–H aliphatic bond. The peak at 1613 cm^{-1} in the monomer spectra shifted to 1680–1645 cm^{-1} in the polymer spectra corresponds to the axial deformation of C=C bonds in aromatic rings, indicating that the aromaticity is preserved in formed polymers. The peak at 1542 cm^{-1} in the monomer spectra shifted to 1515–1564 cm^{-1} in the polymer spectra corresponds to the C–N=C stretching bonds.

SEM. Figure 12 shows the micrographs of the electrodes, recorded after running cyclic voltammetry experiments for uncoated and coated copper and steel by POX. Figures 12a and 12b represent SEM pictures for uncoated copper and steel, respectively. The micrographs show smooth morphology in which clear polishing marks are visible on the surface. Figures 12c and 12d represent SEM micrographs for copper coated with PPOX in the presence of sulfuric acid at different degree of magnifications. The film grown is compact and show a rough surface and globular morphology. Figures 12e and 12f represent SEM micrographs for steel coated with PPOX in the presence of sulfuric acid at different degree of magnifications. The micrographs showed a thick, uniform, smooth, and closely packed continuous film without many holes and scratches and covered the whole steel surface and globular morphology. This films support the results obtained in the cyclic voltammetry techniques and strongly indicated that the PPOX coatings provide improved corrosion protection. In a previous work Pekmez et al. [26] studied the morphologies of the coatings formed by polythiophene and polyaniline on stainless steel surface. The morphologies of polyaniline showed globular surface which by increasing magnification showed nanofiber structure while in case of polythiophene the films showed compact and smooth cauliflower morphology. Also, the polyaniline film was more porous than the polythiophene film. A closer look to the micrographs in this work we can find that the morphology of the films formed is similar to that obtained with polyaniline in Pekmez work. In 2001 Brett compared the morphologies of the films formed by substituted aniline with carboxylic group in poly(aminobenzoic acid) and that obtained in non-substituted aniline [33]. He said that in case of substituted

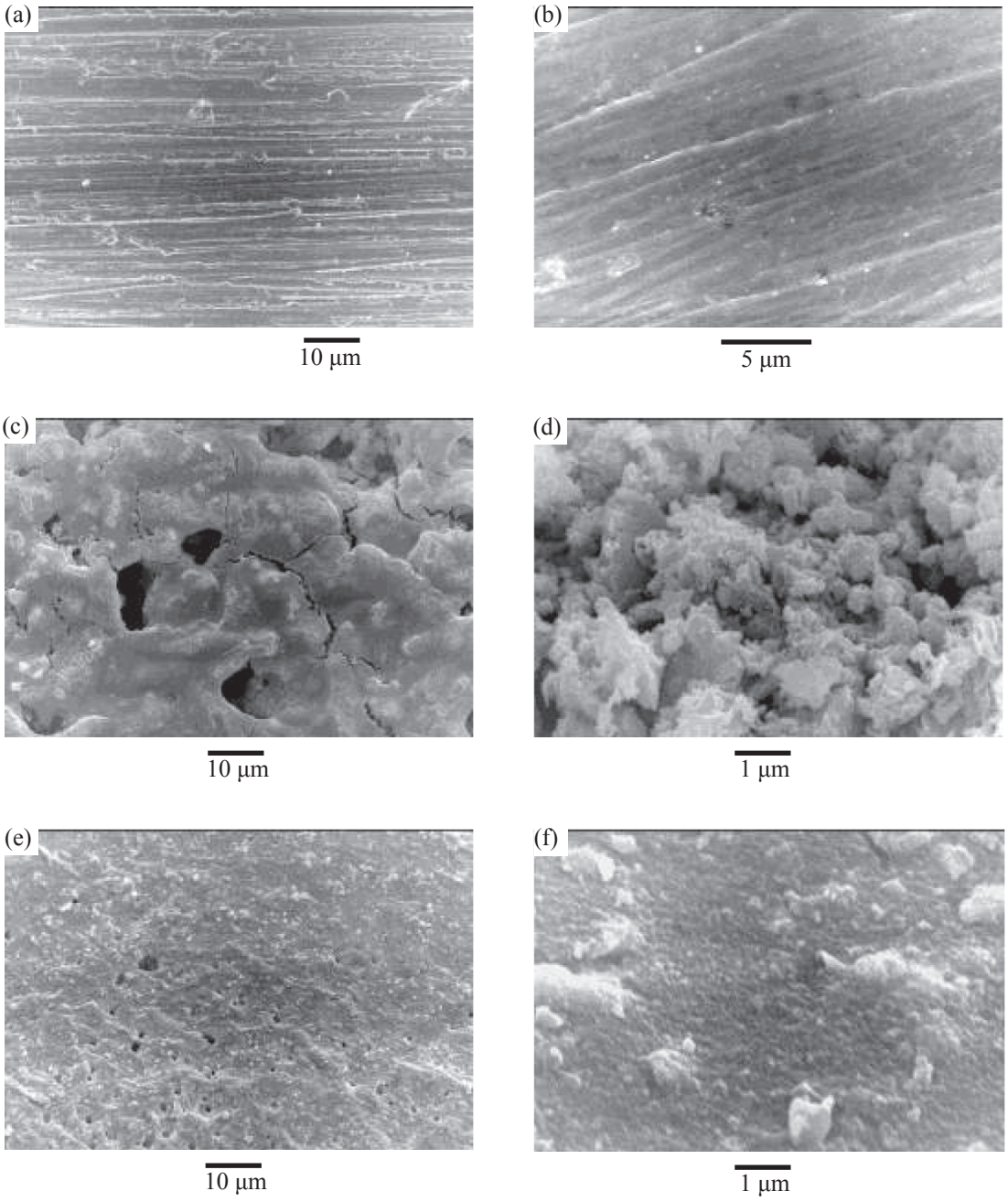

Fig. 12. SEM pictures of (a) uncoated copper; (b) uncoated steel; (c and d) coated copper in the presence of sulfuric acid with different magnifications; (e and f) coated steel in the presence of sulfuric acid with different magnifications.

aniline there is no background film, and a dendrite like film growth occurs at specific sites, while, globular structure is observed in case of non-substituted aniline. He referred the differences in morphologies between the substituted and non-substituted aniline to the different monomer reactivity, short oligomers formed in case of less reactive derivatives. In addition, if the growing polymer is more easily oxidized than the monomer from which it is formed, the less reactive monomer will prefer to react with an already growing polymer rather than the electrode surface leading to weak adhered film [34]. This may explain what happened in this work during the electropolymerization of POX on Cu and Fe in the presence of oxalic acid but with different explanation that the oxalic acid decreases the reactivity of the POX during electropolymerization leading to weak film formed which

is clear from the fact that the intensity of the oxidation peaks in that case increases with the subsequent cycles in Figs. 2 and 4c. We can discuss it in other words, on the basis that the POX monomer is more reactive in low pH in the presence of sulfuric acid than in higher pH in the presence of oxalic acid.

CONCLUSIONS

4-Aminomethyl-5-hydroxymethyl-2-methylpyridine-3-ol is electropolymerized on steel and copper surfaces by cyclic voltammetry.

The film formed in the presence of sulfuric acid on steel and copper is well adhered and show protection performance against corrosion in 0.1 M H_2SO_4.

The FTIR spectrophotometry indicated that both NH_2 and OH function groups participated in the electropolymerization.

The SEM micrographs showed the formation of globular film in case of copper and smooth closely packed and compact film in case of steel.

REFERENCES

1. Mekhalif, Z., Cossement, D., Hevesi, L., and Delhalle, J., *Appl. Sur. Sci.*, 2008, vol. 254, pp. 4056–4062.
2. Liu, M., Wen, Y., Li, D., He, H., Xu, J., Liu, C., Yue, R., Lu, B., and Liu, G., *J. Appl. Polymer Sci.*, 2011, vol. 122, pp. 1142–1151.
3. Patois, T., Lakard, B., Martin, N., and Fievet, P., *Synthetic Metals*, 2010, vol. 160, pp. 2180–2185.
4. Bereket, G., Hur, E., and Sahin, Y., *Appl. Surface Sci.,* 2005, vol. 252, pp. 1233–1244.
5. Nagaoka, T., Kakuno, K., Fujimoto, M., Nakao, H., Yano, J., and Ogura, K., *J. Electroanal. Chem.,* 1994, vol. 368, pp. 315–317.
6. Rose, T.L., D'Antonio, S., Jillson, M.H., Kon, A.B., Suresh, R., and Wang, F., *Synthetic Metals,* 1997, vol. 85, 1439–1440.
7. Mert, B.D., Mert, M.E., Kardas, G., and Yazici, B., *Appl. Surface Sci.*, 2012, vol. 258, pp. 9668–9674.
8. Duran, B., Turhan, M.C., Bereket, G., and Sarac, A.S., *Electrochimica Acta,* 2009, vol. 55, pp. 104–112.
9. Chidsey, C.E.D. and Murray, R.W., *Science*, 1986, vol. 231, pp. 25–31.
10. Abruna, H.D., *Coordination Chem. Rev.,* 1988, vol. 86, pp. 135–189.
11. Dinh, H.N., Renn, X., and Garzon, F.H., *J. Electroanal. Chem.,* 2000, vol. 491, pp. 222–233.
12. Noufi, R.N., Nozik, A.J., White, J., and Warren, L., *J. Electrochem. Soc.,* 1982, vol. 129, pp. 2261–2265.
13. Yu, B. and Khoo, S.B., *Electrochimica Acta,* 2005, vol. 50, pp. 1917–1924.
14. Heinze, J., Frontana-Uribe, B., and Ludwigs, S., *Chem. Rev.,* 2010, vol. 110, pp. 4724–4771.
15. Inzelt, G., Pinerri, M., Schultze, J., and Vorotyntsev, M., *Electrochimica Acta*, 2000, vol. 45, pp. 2403–2421.
16. McCafferty, E., *J. Corrosion Sci.*, 2005, vol. 47, pp. 3202–3215.
17. Popovic, M.M. and Gruger, B.N., *Synthetic Metals*, 2004, vol. 143, pp. 191–195.
18. Pereira da Silva, J.E., *Corrosion Sci.,* 2005, vol. 47, pp. 811–822.
19. Yagan, A., Pekmez, N.O., and Yildiz, A.A., *Progress Organic Coatings*, 2007, vol. 59, pp. 297–303.
20. Inzelt, G., *Conducting Polymers, A New Era in Electrochemistry,* 2012, New York: Springer.
21. Horvat-Raosevic, V. and Kvastek, K., *J. Electroanal. Chem.,* 2006, vol. 591, pp. 217–222.
22. Gospodinova, N. and Terlemezyan, L., *Progress in Polymer Sci*., 1998, vol. 23, pp. 1443–1484.
23. Sadki, S., Schottland, P., Brodie, N., and Sabourand, G., *Chem. Soc. Rev.*, 2000, vol. 29, pp. 283–293.
24. Duran, B., Turhan, M.C., Bereket, G., and Sezai Sarac, A., *Electrochimica Acta*, 2009, vol. 55, pp. 104–112.
25. Muthirulan, P., Kannan, N., and Meenakshisundaram, M., *J. Advanced Research*, 2013, vol. 4, pp. 385–392.
26. Pekmez, N.O., Abaci, E., Cinkilli, K., and Yagan, A., *Progress Organic Coatings*, 2009, vol. 65, pp. 462–468.
27. Pekmez, N.O., Cinkilli, K., and Zeybek, B., *Progress Organic Coatings*, 2014, vol. 77, pp. 1277–1287.
28. Ferreira, C.A., Aeiyach, S., Aaron, J. and Lacasa, P.C., 1996, *Electrochimica Acta*, vol. 41, pp.1801–1809.
29. Ma, H., Chen, S., Yin, B., Zhao, S., and Liu, X., *J. Corrosion Sci.*, 2003, vol. 45, pp. 867–882.
30. Moreira, A.H., Benedetti, A.V., Calot, P.L., and Sumodja, P.T.A., 1993, *Electrochimica Acta*, vol. 38, pp. 981–987.
31. Jinturkar, P., Guan, Y.C., and Han, K.N., *Corrosion*, 1984, vol. 54, pp. 106–114.
32. Wang, D.K.Y., Coller, B.A.W., and Macfarlane, D.R., *Electrochimica Acta*, 1993, vol. 38, pp. 2121–2127.
33. Thiemann, C. and Brett, C.M.A., *Synthetic Metals,* 2001, vol. 123, pp. 1–9.
34. Somasiri, N.L.D. and Macdiarmid, A.G., *J. Polymer Sci.,* 1985, vol. 23, pp. 503–508.